

# Three-Compton Telescope: Theory, Simulations, and Performance

R. A. Kroeger, W. N. Johnson, J. D. Kurfess, B. F. Philips, E. A. Wulf

**Abstract--** The advent of highly segmented gamma ray detectors with good energy resolution has made a new class of gamma ray detectors possible. These instruments record the positions and energies of each individual gamma-ray interaction with high precision. Analysis of the individual interactions can provide energy and directional information, even for events with only partial energy deposition. Advantages over traditional gamma ray detectors include enhanced efficiency, background rejection, gamma ray imaging, and sensitivity to polarization. Consider those gamma rays that interact three or more times in the detector. The energy of the gamma ray that initiated one of these events is uniquely determined by measuring the energies of the first two interactions, and the scatter angle of the second interaction. The precision of this measurement is limited by the energy and position resolution of the detector, but also from Doppler broadening that results from gamma rays scattering off bound electrons in the detector. It is also essential to correctly sequence the first three interactions. The importance of Doppler broadening is greater in higher Z-materials, thus silicon becomes a good choice for the detector material. We discuss performance and simulations of the multiple Compton telescope.

## I. INTRODUCTION

TRADITIONAL gamma ray detectors must completely absorb the energy of a gamma ray in order to determine its energy. A gamma ray may interact several times within the detector before either being completely absorbed in a photo-electric interaction, or possibly escaping the detector. Those gamma rays that escape lead to features such as a Compton shelf below the photo-peak energy, and a loss of photo-peak efficiency. An alternative detection technique is possible in which it is not necessary to fully absorb the gamma ray to determine its full energy. In this approach, a detector must accurately measure the positions and energy

loss of each interaction. A subset of these events will consist of three or more interactions, beginning with two or more Compton events, followed by either a photoelectric event or escaping the detector. The energy of a gamma ray is uniquely determined by the energy loss of the first two interactions, and the scatter angle of the second interaction [1] [2]. We give this process the generic name of “Three-Compton,” referring to the three interactions and the application of the Compton formula to estimate the energy. The energy of the incident gamma ray,  $E_0$ , is given by the formula,

$$E_0 = \Delta E_1 + \frac{\Delta E_2 + \sqrt{\Delta E_2^2 + 4\Delta E_2 m_e c^2 / (1 - \cos \theta_2)}}{2}, \quad (1)$$

where  $\Delta E_1$  and  $\Delta E_2$  are the energy loss of the first and second interaction, and  $\theta_2$  is the Compton scattering angle of the second interaction. Knowledge of the position of first, second, and third interactions is required to determine  $\theta_2$ , however knowledge of the third energy loss is not required. Subsequent interactions are inconsequential if the first three interactions are correctly identified in the proper order. However, additional interactions do contribute to the ability to determine the interaction order without prior knowledge of the sequence.

Three-Compton has several unique properties: (1) efficient detectors in the MeV region are possible using low-Z elements such as silicon, (2) the “Compton shelf” below (or above) the photo-peak is small, especially true for energies above a few 100 keV where the process works best, (3) total energy absorption is not required, and (4) it naturally provides for an imaging gamma ray detector. The Compton shelf from the three-Compton process results from an event where the interaction order is improperly sequenced, or all of the interactions are not correctly resolved and detected. The estimated value for  $E_0$  from Eqn. 1 may therefore be either larger or smaller than the true gamma ray energy in these instances.

The three-Compton process does not require a high-Z detector, *i.e.* high stopping power. In fact, the method requires at least three interactions, thus high-Z materials such as CdZnTe or NaI would not be good choices for energies below around 400 keV, where the probability of photoelectric absorption in the first or second is starting to be either significant or dominant.

We shall not discuss the imaging capability of a Compton telescope here. It is sufficient to note that with the measured

---

This work was supported in part by the Office of Naval Research, the Defence Threat Reduction Agency, and the National Aeronautics and Space Administration.

R. A. Kroeger is with the Naval Research Laboratory, Washington, DC 20375 USA (telephone: 202-404-7878, e-mail: kroeger@nrl.navy.mil).

W. N. Johnson is with the Naval Research Laboratory, Washington DC 20375 (telephone: 202-767-6817, e-mail: johnson@gamma.nrl.navy.mil).

J. D. Kurfess is with the Naval Research Laboratory, Washington DC 20375 USA (telephone: 202-767-3165, e-mail: kurfess@gamma.nrl.navy.mil).

B. F. Philips is with the Naval Research Laboratory, Washington DC 20375 USA (telephone: 202-767-3572, e-mail: philips@gamma.nrl.navy.mil).

E. A. Wulf is with the Naval Research Laboratory, Washington DC 20375 USA (telephone: 202-404-1475, e-mail: wulf@gamma.nrl.navy.mil).

positions of the first and second interactions, and with the measured total energy, the three-Compton detector is an example of a Compton telescope. The first two positions determine the direction of the first scattered gamma ray, and the energy losses provide the scatter angle. The direction of the incoming gamma ray is therefore restricted to a cone, and the superposition of many such event-cones can be used to generate an image. Many examples of Compton telescopes are in the literature, *e.g.* [3].

The efficiency of a three-Compton telescope can be quite high because full-energy detection does not require total absorption. Consequently, the energy of events that would otherwise fall in the Compton shelf of a traditional detector are properly measured with this method. Naturally, the three-Compton telescope must be large enough that the probability of having three interactions is significant.

The determination of the correct order of the interactions for each event is a key factor in efficiency. We presume that direct measurement of event order through fast timing or other techniques is not practical, thus the interaction order must be deduced from the observed energies and positions. Consider, for example, events with exactly three interactions in the detector. There are six possible sequences of these three interactions. Of these, only the correct sequence will provide the correct incoming energy using Eqn. 1, and the correct event-cone for imaging. The other five sequences would provide an erroneous energy and event-cone. Improper sequencing is both a loss of efficiency, and a source of background. In general, there are  $n!$  sequences for events with  $n$  interactions.

The sequencing problem has been studied before for the special case where the full energy of the gamma ray is absorbed. The basic method employs a simple consistency check of energy losses and scatter angles called Compton Kinematics [4]. Recent work by van der Marel et al. [5] search for the interaction that is most probably the terminating photoelectric event, then backtrack the path of the gamma ray to string together the interactions. We shall discuss a simple algorithm to determine the interaction sequence with reasonable to good efficiency. The method makes no assumption concerning total energy absorption or source position.

## II. SIMULATIONS

The incident energy,  $E_0$ , calculated by Eqn. 1 is based on the well-known Compton scattering formula. However, this is only strictly valid for scattering from cold free electrons. In reality, electrons are bound in atoms. The electron momentum affects the scatter angle in a process called Doppler broadening. Doppler broadening contributes an uncertainty in the energy determination [6]. The effect of Doppler broadening is roughly two or three times more significant in higher  $Z$  detector materials such as CdZnTe and Xe, than in lower  $Z$  detectors such as silicon. The limiting energy resolution that can be achieved with ideal silicon

detectors is therefore at least a factor of two better than is possible for ideal CdZnTe detectors [6].

A simple IDL<sup>®</sup> code was developed to perform gamma-ray transport in a Monte-Carlo simulation of simple instrument configurations. The program provides positions and energies of interactions for a simulated beam of gamma rays. It includes the physical processes of gamma-ray cross-sections, ranges, pair production, coherent scattering, Compton scattering and Doppler broadening [7], [8]. It does not propagate recoil electrons, which could become important in thin or low-density detectors, or at high energies. The physics included is sufficient to demonstrate the efficiency, interaction ordering, and energy resolution that can be expected in a realistic instrument.

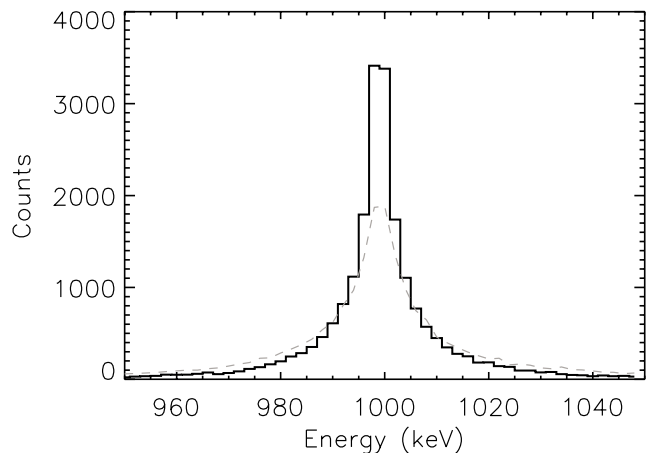


Fig. 1. Reconstructed energy spectrum for a 1 MeV gamma ray beam in silicon. The solid line represents an ideal silicon detector perfect energy and position resolution, and including Doppler broadening. The light dashed curve represents a detector with 2 keV FWHM energy resolution and 2 mm spatial resolution.

### A. Detector resolution

The energy and spatial resolution of the detectors has a significant impact on the accuracy of the energy reconstruction. Fig. 1 shows a reconstruction from simulated data. The two curves are produced from the same data, one with perfect knowledge of energy loss and positions, and the other with the data degraded to represent a realistic detector. Detector energy resolution is presumed to follow gaussian distribution about the true energy, and position resolution is divided into voxels (boxes) with sharp boundaries. The reconstructed energy has a sharp non-gaussian central peak and broad wings, which result from the Doppler broadening in the simulation. We note that the wings of the spectrum representing the realistic detector are reduced if we select only those data where the distance between interactions is a greater than some minimum distance. The appropriate choice of this minimum distance reduces the wings slightly, with little affect on the amplitude of the peak. This is somewhat subjective, and depends on energy and detector properties. Setting the minimum distance too large will cut into the efficiency, though eventually the shape of the distribution will resemble that produced by the perfect data.

## B. Sequencing

Practical 3-Compton detectors are not capable of determining the order of the interactions in each event. This was done in COMPTEL by fast timing between detectors 1.5 meters apart [3]. The 3-Compton telescope is presumed to bring the detectors into close proximity in order to increase the efficiency, thus light propagation times are much shorter. Further, the fast timing possible in COMPTEL would require far more power and/or significant advances in detector technology with the segmented semiconductors considered for this application. Thus, the event order must be determined by observing the pattern and amounts of energy losses within the detector.

Consider those events with exactly three interactions. There are six possible permutations in which to order these interactions. Once a trial sequence is determined, the energies and angles of the trial gamma ray are determined. The sequence with the correct order will be fully consistent with Compton kinematics. A simple way to test a sequence is to apply Eqn. 1 to find an energy,  $E_0$ , for that sequence. Two tests can be applied: (1) is the first measured energy loss,  $\Delta E_1$ , a valid Compton scatter value, given an incident energy of  $E_0$ ? An example of a rejected sequence might reconstruct to 1 MeV, with an initial energy loss of 0.90 MeV, and a scattered gamma ray of 0.10 MeV. Clearly this is then inconsistent with the maximum energy loss of 0.80 MeV from a 180-degree Compton scatter, and therefore is not physical. (2) The third interaction of a valid sequence must be consistent with either a final Compton scatter *or* a total energy absorption in a photoelectric interaction.

Tie-breakers can be resolved by application of a score, or Figure of Merit (FOM) that is computed for each valid sequence. Possible FOM terms are derived from the product of probabilities of the chain of events in the sequence. These may include the Klein-Nishina differential cross-section for each scatter angle,  $\theta_i$ , and energy loss  $\Delta E_i$ ,

$$FOM_i = \frac{d\sigma}{d\Omega}(\theta_i, \Delta E_i), \quad (2)$$

thus rare scatter angles would be given lower weight. The FOM may also consider other factors such as the range probabilities for each gamma ray in the sequence,

$$FOM_j = e^{-\sigma(E_j)x_j}, \quad (3)$$

where  $x_j$  is the distance between two interactions,  $E_j$  is the energy of the gamma ray that connects them, and  $\sigma$  is the total cross-section. It is also possible to apply Eqn. 3 to range of the first or last interaction to the entry or exit points of the detector, although this is more complicated since the incoming and exit directions may not be known. The best reconstruction strategy and FOM for a given instrument, energy, or other variables lends itself well to Monte Carlo analysis.

Giving preference to those sequences that end with a photoelectric event provides a third useful factor. The photoelectric cross-section for the final interaction may well

be smaller than the corresponding Compton cross section. However, the probability of an interaction landing in the narrow energy window that defines a photoelectric ending is relatively small. Thus, this tends to be a powerful discriminator. An effective photoelectric weighting factor is to increase the FOM for a sequence by 10% if it is consistent with total energy absorption. The algorithm is not sensitive to the precise value of this weighting factor. Photoelectric sequences are of particular interest, as the more accurate energy determination is usually to sum the measured energy losses, rather than the application of Eqn. 1.

The effectiveness of sequencing the algorithm was studied using the simulated data from a large silicon detector. The algorithm used for three interactions employs the differential cross-section terms from Eqn. 2, a physical consistency check on the first and last interactions, and photoelectric weighting term.

Our algorithm was able to identify the correct sequence 40%, 47%, and 80% of the time at 185, 414, and 2615 keV respectively for three interactions. The remaining 60%, 53%, and 20% of the sequences, respectively were incorrectly sequenced, thus contribute to background and should not be included in the estimate of detection efficiency.

We note that the range probability FOM given by Eqn. 3 does not help in the three-interaction example. Improper sequences often reconstruct to higher energies, and higher energy gamma rays have longer ranges. Thus the range statistic prefers to select higher-energy solutions. The range statistic does improve sequencing slightly with four or more interactions. It is likely to be more effective in sequencing problems with additional boundary conditions such as known source position, incident energy, or terminating interaction.

Another powerful term is added to the FOM with four or more interactions. Consider four interactions: an incident energy is determined using Eqn. 1 for the first three interactions, and an independent energy is calculated using the last three interactions (the energy  $E_1$  is determined from the last three interactions through Eqn. 1 in much the same manner as  $E_0$  is determined from the first three interactions.  $E_0$  is then found by adding the first energy loss,  $\Delta E_1$ ). These two determinations of  $E_0$  should be the same within a reasonable error window. There are 24 possible sequences for four interactions. Most of these invalid sequences are easily excluded by thus this additional term. This procedure is essentially the same as the Compton Kinematic approach described by Aprile [4], only without the assumption of total energy absorption of the incident gamma ray.

Our algorithm was able to identify the correct sequence 45%, 64%, and 87% of the time at 185, 414, and 2615 keV, respectively for events with four interactions.

This approach easily generalizes to five or more interactions. Each sequential set of three interactions is an independent estimate of energy, and they must all be self-consistent. Each sequence is assigned a FOM component based on the difference between each estimator of energy, and

the sequence with the highest over-all FOM is selected as “best.” Event ordering is computationally limited above about six interactions. There are 720 possible sequences with six interactions, each of which must be evaluated to determine the best. Presently, we reject events with seven or more interactions until a more sophisticated algorithm can be developed to limit the search.

### C. Realistic Detectors

Energy resolution and position resolution degrade the accuracy of both the reconstructed energy and the sequencing efficiency. This is shown in Fig. 2 for various values of detector position resolution. A detector energy resolution of 2 keV FWHM was used. Reconstructed energy resolution used in the Figure is the Full-Width Half Maximum of the energy distribution. This is coincidentally similar to the width that contains 50% of the peak area due to the non-gaussian peak shape for detector energy resolutions in the range 4 – 10 keV FWHM.

It is evident that position resolution has the most effect on reconstructed energy resolution at higher energies. This means that detectors of higher average density with correspondingly shorter gamma ray ranges require correspondingly more accurate position information to achieve similar performance as lower average density detectors. We note that the detectors in this simulation were 7 mm thick with 13 mm gaps between them, with an average density of  $0.8 \text{ g/cm}^3$ . A fair metric to compare detector spatial resolution is a normalized value equal to the position resolution times the average density. Thus, a silicon device in this simulation with 2 mm spatial resolution has a normalized position resolution of  $0.16 \text{ g/cm}^2$ . A similar sensitivity to position resolution could be achieved using 6 mm thick germanium detectors with 1 mm spatial resolution spaced on the same 20 mm pitch. This device would have an average density of  $1.6 \text{ g/cm}^3$  and a normalized position resolution of  $0.16 \text{ g/cm}^2$ .

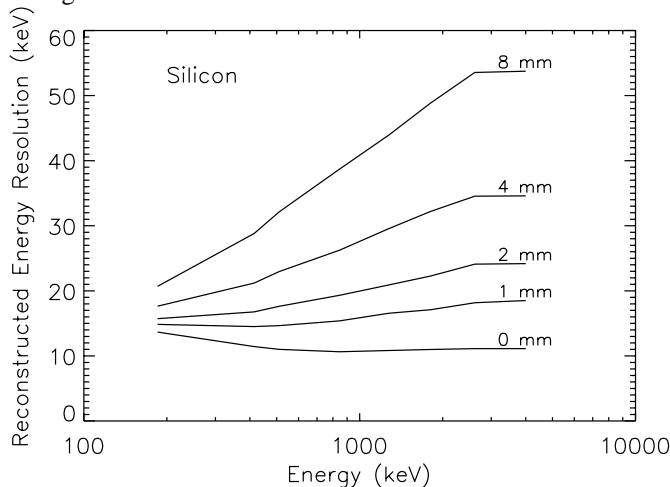


Fig. 2. Reconstructed energy resolution vs. incident energy for various detector voxel sized (position resolution). The detector energy resolution is 2 keV FWHM.

Detector energy resolution is also a key factor in the reconstructed energy resolution as shown in Fig. 3, particularly for detectors that have very good spatial resolution (*i.e.* a normalized spatial resolution less than about  $0.16 \text{ g/cm}^2$ ). A silicon detector with 2 mm spatial resolution and 2 keV FWHM energy resolution should achieve 15 keV FWHM reconstructed energy resolution at 511 keV. If the detectors, instead, have resolution 6 keV FWHM, they should achieve a reconstructed resolution of 19 keV FWHM, only slightly worse. The latter instrument may be easier to build into large areas. Another interesting comparison: a detector with 4 mm spatial resolution and 2 keV FWHM would achieve roughly the same reconstructed energy resolution as a detector with 2 mm spatial resolution and 6 keV FWHM at 511 keV.

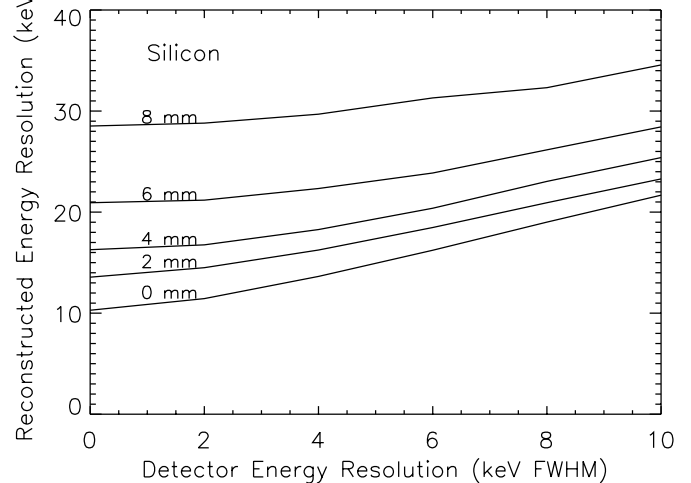


Fig 3. Reconstructed energy resolution vs. detector energy resolution for 0.511 MeV gamma rays. The various curves indicate position resolution of the detectors.

The relative importance of energy resolution and spatial resolution depends on incident energy. A general rule: energy resolution in the range of 0 – 10 keV is the dominant parameter at incident energies below 0.5 MeV, and position resolution in the normalized range of 0 –  $0.64 \text{ g/cm}^2$  is the dominant parameter above about 0.5 MeV.

### III. EFFICIENCY

The efficiency of a three-Compton telescope is limited by a combination of: a) size of the detector, b) producing three or more detectable interactions, c) properly sequencing the event order, d) passive materials within the detection volume where key interactions may be lost, and e) no more than six interactions with our present computer power and algorithm. Fig. 3 shows the expected efficiency after pulling all of these factors together for a  $1 \text{ m}^2$  area detector, with a total thickness of  $43 \text{ g/cm}^2$ .

A detection threshold of 10 keV was used, thus coherent scatters and very small angle Compton scatter events are not detected. Events with undetected interactions constitute one component of lost efficiency. The low threshold is most significant for lower energy gamma rays where coherent and

low energy-loss Compton scattering is more likely. The importance of the detection threshold at 1 MeV is significant. 17% of the three-or-more interaction events in a simulation of a silicon instrument have at least one of the first three interactions less than 10 keV, and thus lost in the three-Compton reconstruction. The loss rises to 29% for a 20 keV detection threshold, and 49% for a 40 keV detection threshold. The efficiency loss due to the detection threshold is worse toward lower energies. At 511 keV, 27% of the events are below a 10 keV detection threshold.

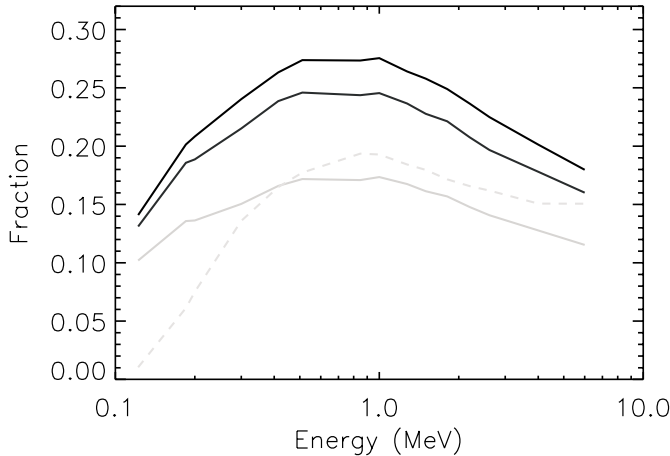


Fig. 4. Efficiency of a 3-Compton telescope vs. energy. The three solid curves are for a silicon detector, the dashed curve is for germanium. The upper curve shows the fraction efficiency for an ideal silicon detector with perfect position and energy resolution. The next curve below this shows the same detector with 3 keV FWHM energy resolution and 1 mm voxel resolution. The lower solid curve represents this detector with 10% passive materials. The dashed curve is for a similar sized germanium detector with realistic resolution and 10% passive materials. The efficiency for a standard 2-interaction Compton telescope is not shown. This will significantly enhance the germanium efficiency for the lower energies.

There is potential improvement in the efficiencies shown in Fig. 4 by utilizing those events with 7 or more interactions. A potential gain of around 50% is possible for the silicon curves at high energies (roughly 1 MeV and above) by this improvement alone. It may also be possible to further improve the sequence selection algorithm. Presently we only count valid sequences to determine efficiency, however a fair number of five and six interaction sequences have the first three and most critical interactions sequenced correctly. What happens after the third interaction need not invalidate a sequence.

Efficiency of the silicon 3-Compton telescope could also be improved by considering a hybrid instrument that includes thin layers of a high-Z detector such as CdZnTe. The CdZnTe would increase the probability of absorbing low energy photons toward the end of the sequence, and reduce the total number of interactions in the sequence.

#### IV. CONCLUSIONS

The simulated three-Compton efficiency shown in Fig. 4 is well over an order of magnitude higher than the slightly larger COMPTEL instrument on the *Compton* Gamma Ray

Observatory. Efficiency also extends to much lower energies than does COMPTEL. The reasons for improvement are simple: more compact geometry, ability to utilize a much larger fraction of the events, including those that are not total absorption events, and ascribing no significance to where in the detector that the first interaction occurs. In contrast, COMPTEL required that the first interaction be in the upper detectors. The lower energy performance is largely a matter of using low noise semiconducting detectors to initially scatter the gamma ray vs. liquid scintillators used in COMPTEL.

Also, COMPTEL primarily relied on scatters of less than roughly 30 degrees in the first interaction, further reducing their efficiency. The restriction on the first scatter angle helped exclude background events consistent with originating from far off axis, in this case from the Earth or spacecraft. Presumably an Advanced Compton Telescope (ACT) using the three-Compton principle and operating in a similar environment would also have to exclude some fraction of events that could have originated from below the instrument. Unlike COMPTEL, the ACT should be able to keep those large scatter events where the downward portion of the event-cone has a significant path through the detectors. In effect, a large ACT provides the its own shielding for gamma rays from below. It may also be practical to consider shielding below or the sides of a smaller ACT design.

The sequencing algorithm may be improved slightly. The optimum FOM may be determined through additional Monte Carlo simulations. Improvements are possible by fine-tuning the FOM as a function of energy, or by prior knowledge about the source.

Applications that require a large, imaging field of view are likely to benefit from the three-Compton approach. These include astrophysics where long integration times and full-sky coverage are essential to capture faint and transient events such as supernovae explosions. This may also be applicable in survey applications where imaging may help isolate radioactive hot spots, and reduce susceptibility to ambient backgrounds.

#### V. REFERENCES

- [1] J. D. Kurfess, W. N. Johnson, R. A. Kroeger and B. F. Philips, "Considerations for the next Compton telescope mission", *AIP Conf. Proc.* 510, pp. 789-793, 2000.
- [2] N. Dogan and D.K. Wehe, "Optimization and Angular Resolution Calculations for a Multiple Compton Scatter Camera," *Nucl. Sci. Symp & Medical Imaging Conf.*, Vol. 1, pp 269-273, 1993.
- [3] V. Schönfelder, H. Aarts, K. Bennett, H. de Boer, J. Clear, W. Collmar, et al., "Instrument description and performance of the imaging gamma-ray telescope COMPTEL aboard the Compton Gamma-Ray Observatory," *ApJS*, Vol. 86, pp. 657-692, 1993.
- [4] E. Aprile, A. Bolotnikov, D. Chen, and R. Mukherjee, "A Monte Carlo analysis of the liquid xenon TPC as gamma-ray telescope," *Nucl. Instr. And Meth.*, A 327, pp. 216-221, 1993
- [5] J. van der Marel and B. Cederwall, "Backtracking as a way to reconstruct Compton scattered  $\gamma$ -rays," *Nucl. Instr. And Meth.*, A 437, pp. 538-551, 1999
- [6] Y.F. Du, Z. He, G.F. Knoll, D.K. Wehe, W. Li, "Evaluation of a Compton scattering camera using 3-D position sensitive CdZnTe detectors," *Proc. SPIE*, vol. 3768, pp. 228, 1999.

- [7] Y. Namito, S. Ban, H. Hirayama, "Implementation of the Doppler broadening of a Compton-scattered photon into the EGS4 code," *Nucl. Instr. And Meth.*, A 349, pp. 489-494, 1994.
- [8] F. Biggs, L.B. Mendelsohn, J.B. Man, "Hartree-Fock Compton profiles for the elements," *Atomic Data and Nucl. Data Tables*, 16, pp. 201-309, 1975.